

# Ionized iron $K\alpha$ lines in AGN X-ray spectra

Stefano Bianchi and Giorgio Matt

Dipartimento di Fisica, Università degli Studi Roma Tre, Via della Vasca Navale 84, I-00146 Roma, Italy

Received ; accepted

**Abstract.** The Equivalent Widths (EW) of the He– and H–like iron lines produced in photoionized, circumnuclear matter of AGN are calculated with respect to both the reflected and the total continua. We found that the EWs with respect to the total continuum may be as large as a few tens of eV, making them observable in bright Seyfert 1s by instruments on board *Chandra* and *XMM–Newton*. We apply our calculations to the *XMM–Newton* spectrum of NGC 5506 and found a good agreement with the data at the expense of a modest iron overabundance.

**Key words.** Line: formation; Galaxies: individual: NGC 5506 – Galaxies: Seyfert – X-rays: galaxies

## 1. Introduction

The basic idea behind unification models for Seyfert galaxies is that all objects are intrinsically the same and all observed different features are simply the result of the orientation of the system with respect to the line of sight.

In this scenario, emission from circumnuclear regions is much easier to observe in Seyfert 2s (and in particular in Compton–thick ones), where the nuclear radiation is obscured, than in unobscured Seyfert 1s in which these components are heavily diluted by the photons from the nucleus. Indeed, such regions are commonly observed in Seyfert 2s (e.g. Matt 2001 for a review), and found to be of at least two types: a cold gas with high column density which partially or completely obscures the nuclear radiation (the ‘torus’) and an ionized, optically thin medium that scatters it into the line of sight. Both these materials produce a reflected continuum and narrow iron  $K\alpha$  lines (e.g. Matt et al. 1996, hereinafter MBF96).

If these emitting regions are also present in the environment of Seyfert 1s, as expected in unification schemes, we should in principle be able to observe these lines as well, although with a much smaller EW due to the dilution by the direct nuclear continuum. The limited sensitivity and energy resolution of past X–ray missions prevented, until a couple of years ago, the unambiguous detection of these features in unobscured sources. The situation has been radically changed with the launch of *Chandra* and *XMM–Newton*. Indeed, a narrow neutral iron line have been found to be fairly common in Seyfert 1s spectra (e.g. Kaspi et al. 2001; Yaqoob et al. 2001; Weaver 2002; Yaqoob et al. 2002 for *Chandra* results; Reeves et al. 2001; Pounds et al. 2001; Gondoin et al. 2001; Matt et al. 2001

for *XMM–Newton* findings). On the other hand, evidence for ionized iron  $K\alpha$  lines at 6.7 and 6.96 keV from distant matter have been reported so far in only one unobscured (at the lines energies) Seyfert, namely NGC 5506 (Matt et al. 2001).

In this paper, we calculate the expected equivalent widths for the two ionized lines with respect to both reflected and total continua. Details of the calculations and results will be presented in Sects. 2 and 3, respectively, and the case of NGC 5506 discussed in Sect. 4.

## 2. The model

The line emitting material is assumed to be optically thin to Thomson scattering and in photoionization equilibrium, as observed e.g. in the ‘hot reflector’ in NGC 1068 (see Guainazzi et al. 1999; Bianchi et al. 2001). In these conditions, both recombination and resonantly scattered  $K\alpha$  lines from H– and He–like iron ions can be produced.

Resonantly scattered  $K\alpha$  lines consists of radiative de–excitation following excitation from continuum photons. The radiative channel has a probability of occurrence which, for Fe xxv and Fe xxvi, is unity as Auger de–excitation is of course impossible. The angular dependence of the emission depends on the transition involved (Chandrasekhar 1960). In the column density intervals explored in this paper, resonant lines are optically thick. Therefore, the first resonant scattering occurs preferentially close to the illuminated surface (this effect of course becoming more and more important as the column density of the matter increases). As there are not competing processes apart from Compton scattering (which has a much smaller cross section), the line photons eventually escape from the matter, but with a larger probability to escape from the illuminated surface (reflection case, see

Fig. 1) rather than from the opposite boundary (transmission case). Line transfer in the matter is treated here by means of Monte Carlo simulations.

Recombination  $K\alpha$  lines occur after a photoionization of a K shell electron. Similarly to the case of fluorescence, it is customary to describe the process by introducing an effective fluorescent yield  $Y$ , which is the probability that the recombination cascade does include the  $K\alpha$  transition (Krolik & Kallman 1987; MBF96). Recombination occurs almost homogeneously in the matter, as it follows photoabsorption, which is optically thin in the column density ranges considered here. Of course,  $K\alpha$  line photons produced by recombination may in turn be resonantly scattered before escaping, but because of the uniform source function there is no preferred escaping surface. This process can be therefore treated in the optically thin approximation, thus analytically.

Both processes and their treatment are described in detail in MBF96, to which the reader is deferred.

Ionization fractions for Fe XXV and Fe XXVI have been calculated with the well known public photoionization code CLOUDY<sup>1</sup> (v94.00; Ferland 2000), as a function of the ionization parameter  $U$ , defined as:

$$U = \frac{\int_{\nu_R}^{\infty} \frac{L_{\nu}}{h\nu} d\nu}{4\pi r^2 c n_e} \quad (1)$$

where  $c$  is the speed of light,  $r$  the distance of the gas from the illuminating source,  $n_e$  its density and  $\nu_R$  the frequency corresponding to 1 Rydberg. This, however, is not the best choice when investigating highly ionized iron atoms, as the result depends dramatically on the spectral shape of the photoionizing continuum. Assuming a power law shape, a small change in the spectral index (for the same  $U$ ) may change significantly the number of X-ray photons (which are the most relevant in this case). We decided to use instead a ‘‘X-ray’’ ionization parameter, defined over the 2–10 keV energy range:

$$U_x = \frac{\int_2^{10} \frac{L_{\nu}}{h\nu} d\nu}{4\pi r^2 c n_e} \quad (2)$$

where the integration limits are the frequencies correspondent to 2 and 10 keV. The conversion factor between the two ionization parameters is clearly a function of the power index of the continuum:

$$\frac{U_x(\gamma)}{U} = \frac{\int_2^{10} \frac{L_{\nu}}{h\nu} d\nu}{\int_{\nu_R}^{\infty} \frac{L_{\nu}}{h\nu} d\nu} = -\frac{10^{1-\gamma} - 2^{1-\gamma}}{E_R^{1-\gamma}} \quad (3)$$

where  $\gamma$  is the photon index of the powerlaw and  $E_R = 13.6 \times 10^{-3}$  keV. Adopting this new definition of the ionization parameter, the results are almost independent of  $\gamma$ : the residual effects will be presented at the end of the next section, together with those due to changing the temperature and density of the gas.

<sup>1</sup> <http://www.pa.uky.edu/~gary/cloudy/>

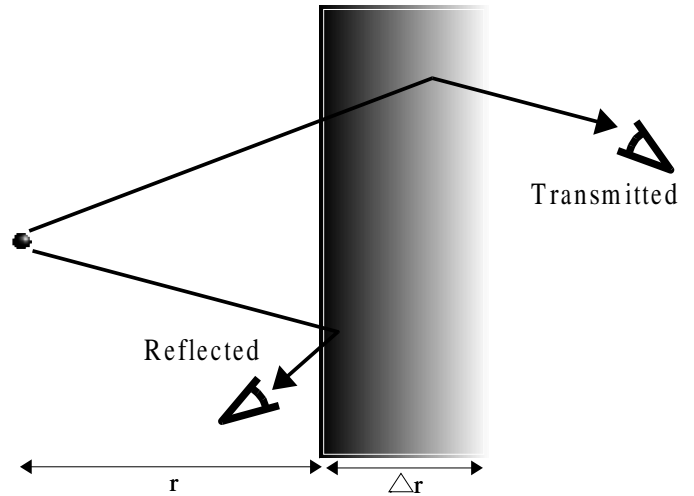


**Fig. 1.** The adopted geometry.

The sketch in Fig.1 shows the geometry adopted in our calculations. We assumed  $\Delta r=r$  and isotropic illumination within a  $30^\circ$  cone. As said above, the equivalent widths of the resonant scattered lines are different when transmitted or reflected spectra are considered. Therefore, we will present plots for both cases.

### 3. Results

In Figs. 2, 3, 4 and 5 the equivalent widths of Fe XXV and Fe XXVI  $K\alpha$  lines (recombination plus resonantly scattered; hereinafter we will always consider the sum of the two contributions) against the transmitted (or reflected) continuum only are plotted as a function of  $\log U_x$  and for different values of the column densities of the line emitting gas. The results are obtained with  $\gamma = 2.0$ ,  $T = 10^6$  K,  $n_e = 10^6 \text{ cm}^{-2}$ . Plots in Figs. 2 and 3 were obtained combining the results in figure 4, 5 and 6 of MBF96 (where EWs of recombination and resonant lines were presented assuming ionization fractions equal to 1 for the interested ion) with the ionization structures calculated by CLOUDY as a function of  $U_x$ . The iron abundance is assumed equal to the solar one (as for Morrison & McCammon 1983). As described in MBF96, for small column densities the main contribution comes from the resonant lines, while at large column densities recombination dominates, because photoionization is still optically thin while resonant scattering is thick, and the line production for the latter process consequently saturates. Plots in Figs. 4 and 5 have been obtained re-running the Monte Carlo code described in MBF96 for a reflecting, rather than transmitting, material. Because the two cases differs only for the contribution of the resonant lines, the main differences occur for small column densities.

In Figs. 6 and 7 the EWs, obtained for the reflecting matter, are instead calculated against the total continuum. (The corresponding plots for the transmitted flux are not shown because differences are appreciable only for small column densities, where the EWs are very small.)

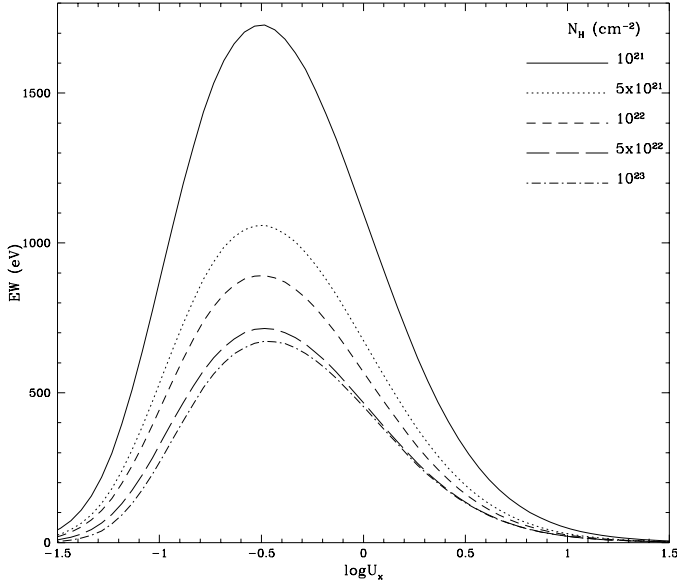


**Fig. 2.** Fe XXV EWs against transmitted continuum only as a function of  $\log U_x$  and column density.

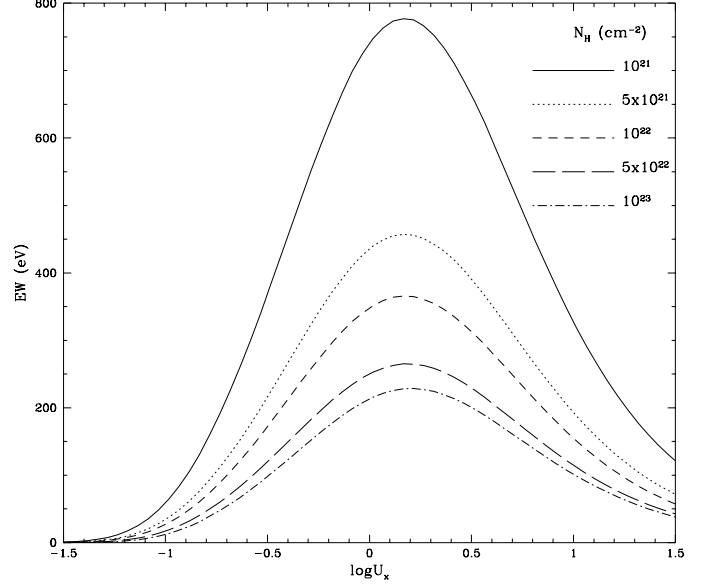


**Fig. 3.** Fe XXVI EWs against transmitted continuum only as a function of  $\log U_x$  and column density.

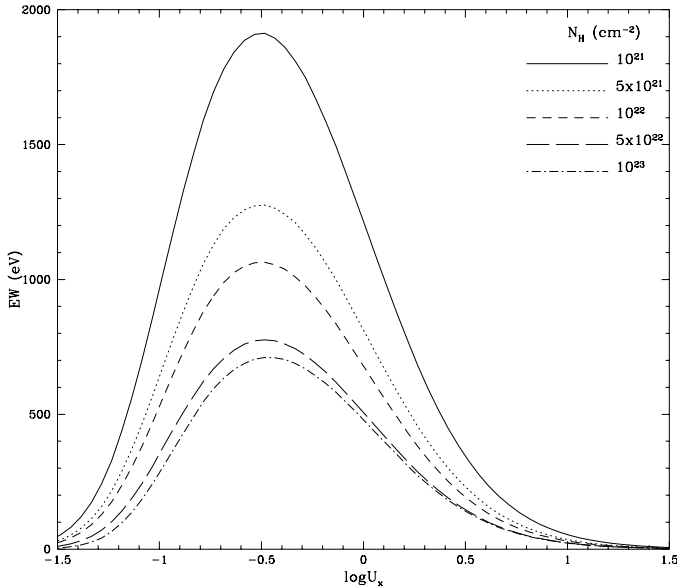


**Fig. 4.** Fe XXV EWs against reflected continuum only as a function of  $\log U_x$  and column density.

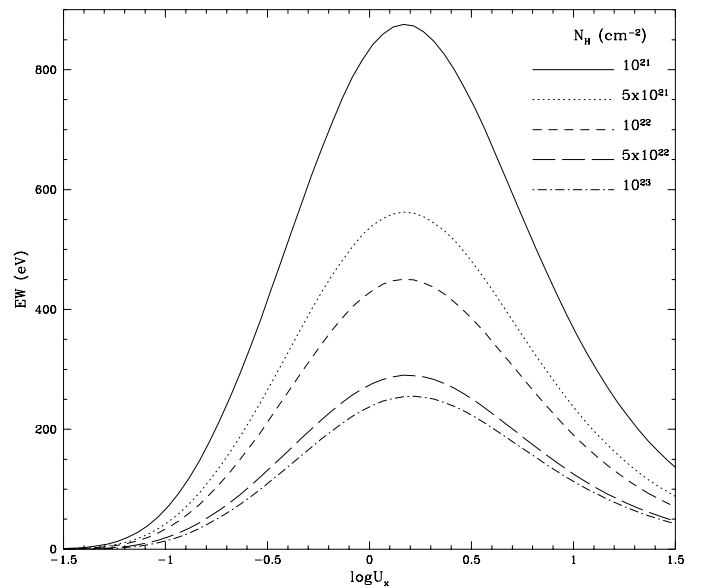


**Fig. 5.** Fe XXVI EWs against reflected continuum only as a function of  $\log U_x$  and column density.

The relation between the EWs with respect to reflected and total continua is easy to calculate. In the Compton-thin regime, the reflected flux is given by:

$$F_r \simeq f \cdot \tau \cdot F_t \quad (4)$$

where  $F_t$  is the illuminating flux and  $f$  a geometrical factor (basically the solid angle subtended by the illumi-

nated matter);  $\tau = \frac{N_H}{1.5 \times 10^{24}}$  is the Thomson optical depth. Therefore, the equivalent widths are:

$$EW_t = EW_r \cdot \frac{F_r}{F_t + F_r} \simeq EW_r \cdot \frac{F_r}{F_t} \simeq EW_r \cdot f \cdot \tau \quad (5)$$

Figs. 6 and 7 have been obtained assuming  $f=1$ .

Finally, we illustrate the effects of changing the value of  $\gamma$ ,  $T$  and  $n_e$ . Fig. 8 shows the equivalent widths of

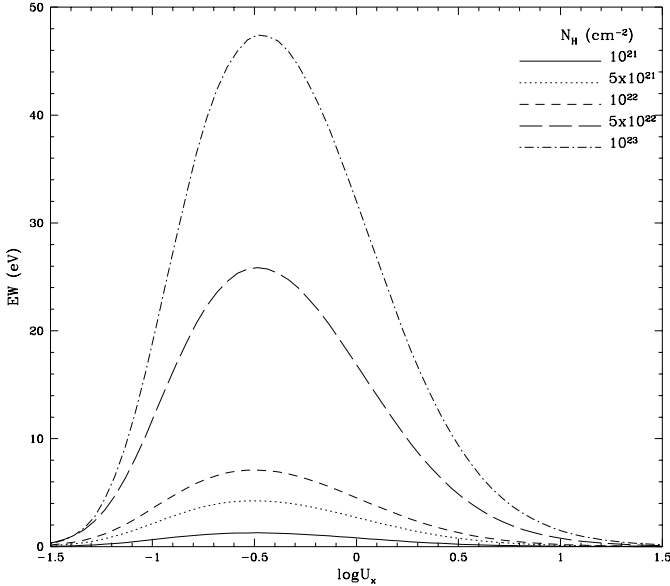


**Fig. 6.** Reflected Fe XXV EWs against total continuum as a function of  $\log U_x$  and column density ( $f=1$ : see text for details).

Fe XXV lines against the total continuum for a column density of  $10^{23} \text{ cm}^{-2}$  and different values of the photon index of the incident continuum. Clearly, the choice of  $U_x$  instead of  $U$  keeps the differences small: the maximum of the function occurs almost at the same value of  $U_x$  for the various indices, while it would have been significantly shifted if plotted against  $U$ . There is however a difference in the value of the maximum, which increases with  $\gamma$ .

The opposite occurs for Fe XXVI (Fig. 9), with a shift in the value of  $U_x$  for which the function has the maximum value, but not appreciable differences in the values of this maximum.

The effect of changing the gas temperature is shown in Figs. 10 and 11. The overall result is, as expected, that the colder is the gas the higher is the ionization parameter required to reach the peak in the ionization fraction of both the iron ions. On the other hand, there are no significant changes in the maximum values of the equivalent widths of the lines.

A change of the gas density over a wide range ( $10^4 - 10^8 \text{ cm}^{-3}$ ) does not instead produce any appreciable variations in our results. This is expected, because the ionization parameter is a quantity that describes the ionization structure of a gas under a combination of density, distance and luminosity of the incident radiation. Changing one of these quantities keeping the ionization parameter fixed ends up only in a rescale of the other ones, without changing the ionization structure of the gas surface.

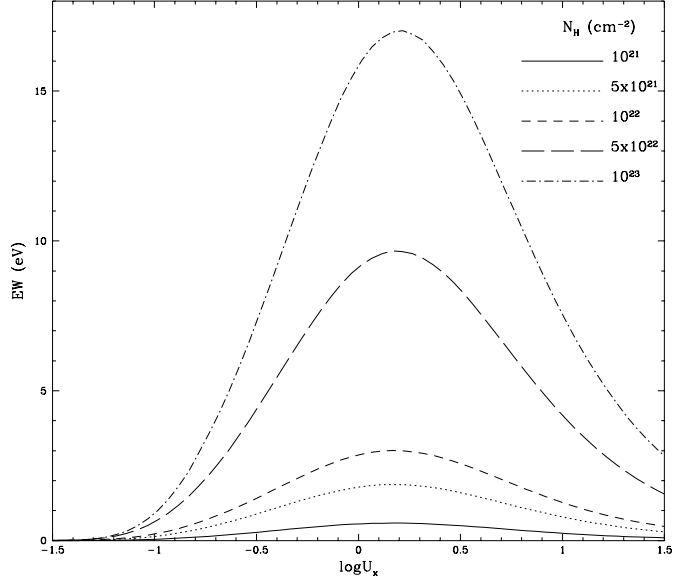


**Fig. 7.** Reflected Fe XXVI EWs against total continuum as a function of  $\log U_x$  and column density ( $f=1$ : see text for details).

#### 4. An example: NGC 5506

Let us now compare our calculations with the only case in which the presence of ionized iron  $K\alpha$  lines from circumnuclear matter have been claimed in an unobscured (at the iron line energies) source, namely NGC 5506 (Matt et al. 2001).

NGC 5506 is a bright Narrow Emission Line Galaxy, optically classified as an intermediate Seyfert with a highly reddened BLR (Veron-Cetty & Veron 2001). Several X-ray observations clearly indicate the presence of a hidden Seyfert 1 nucleus (Matt et al. 2001 and references therein). Its iron  $K\alpha$  line has been claimed to be complex by *ASCA* (Wang et al. 1999) and *RXTE* (Lamer et al. 2000) observations. *BeppoSAX* found an iron line centroid energy definitely higher than 6.4 keV (Perola et al. 2002).

XMM-*Newton* data definitely confirm that the iron line is complex, with at least two components clearly present: one narrow, corresponding to neutral iron, the other broad and consistent with ionized iron.

Even if a fit of the ionized, broad component with a disc relativistic line is as good as that with a blend of He- and H-like unresolved lines, the second solution is preferable from a physical point of view, as argued by Matt et al. (2001). If this is, indeed, the case, these two lines are likely to be produced in a photoionized matter as the one described in this paper. The observed equivalent widths are  $40 \pm 16 \text{ eV}$  and  $32 \pm 15 \text{ eV}$  for Fe XXV and Fe XXVI, respectively.

Moreover, NGC 5506 presents a soft excess whose normalization is about 2% of the primary component: recalling equation (4) this could be the result of reflection from

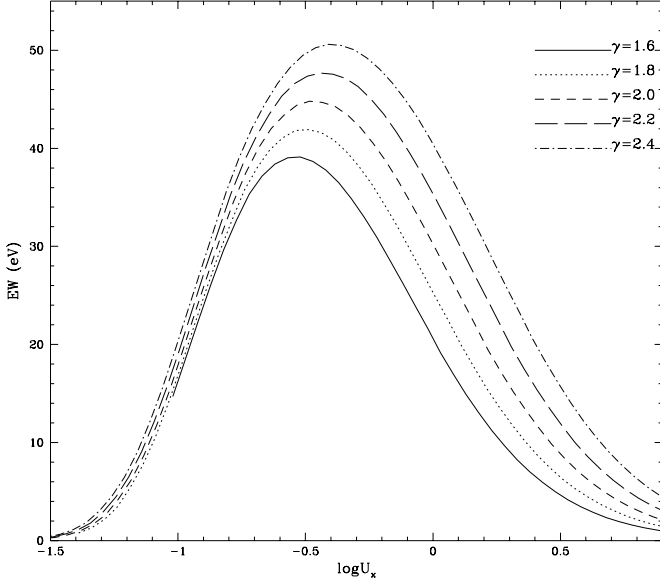


**Fig. 8.** Fe XXV EWs against total continuum for different values of  $\gamma$ . Column density is  $10^{23} \text{ cm}^{-2}$ .

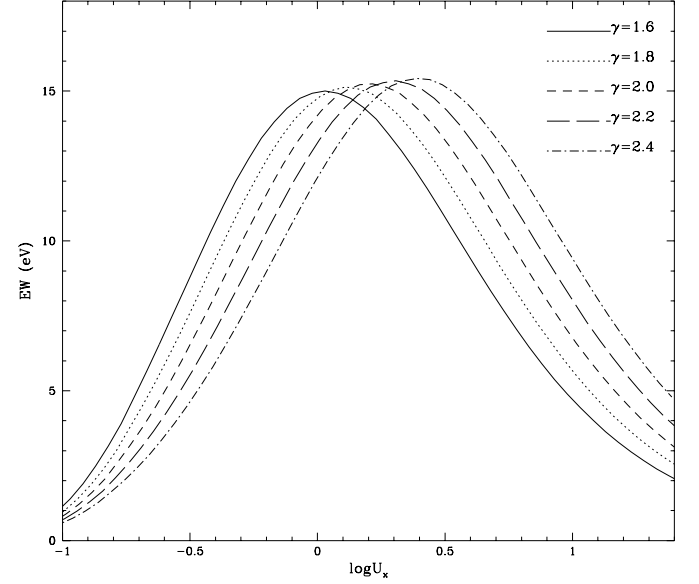


**Fig. 9.** Fe XXVI EWs against total continuum for different values of  $\gamma$ . Column density is  $10^{23} \text{ cm}^{-2}$ .

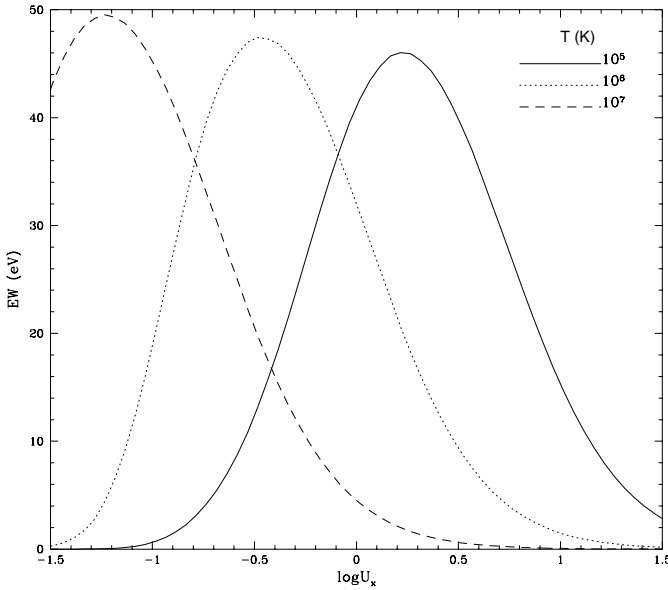


**Fig. 10.** Fe XXV EWs against total continuum for different values of  $T$ . Column density is  $10^{23} \text{ cm}^{-2}$ .

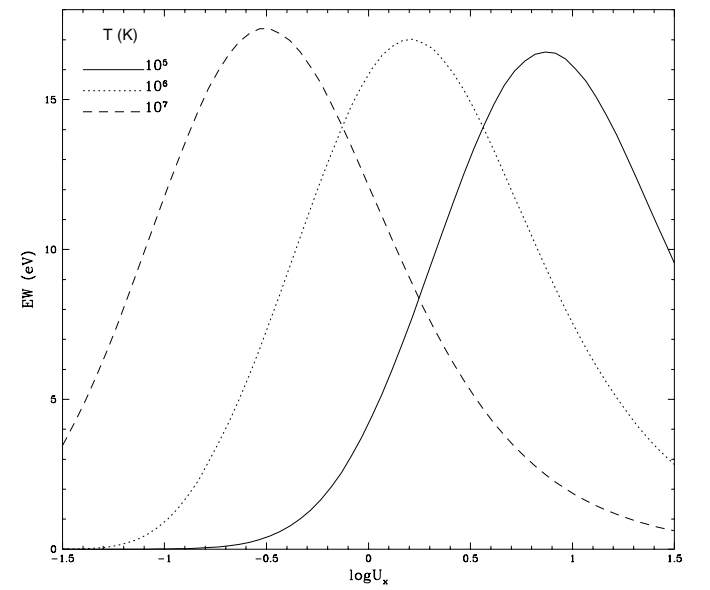


**Fig. 11.** Fe XXVI EWs against total continuum for different values of  $T$ . Column density is  $10^{23} \text{ cm}^{-2}$ .

a gas with column densities of  $3 \times 10^{22}/f \text{ cm}^{-2}$ . Let us now assume that the two ionized lines and the soft X-ray emission come from one and the same matter. Let us also assume  $f=1$  (a smaller value of  $f$  would imply a larger value of the column density to produce the observed flux of the reflected continuum: the two parameters have the same effect on the line EWs, and in the first approxima-

tion we can assume that the EWs are almost independent of their ratio). The observed EWs can be reproduced provided that  $\log(U_x) \sim 0 \div 0.5$  ( $T = 10^6 \text{ K}$ ) and the iron is overabundant by a factor  $2 \div 3$ . (A different choice of the gas temperature would require a different value of  $\log(U_x)$ , but not of the iron abundance, see Figs. 10 and 11). This solution is of course valid in the stationary case. If the

source flux was larger in the past than during the XMM–*Newton* observation, then the requirement on the iron overabundance will be correspondingly reduced; it is worth noting that the flux during the XMM–*Newton* observation was about 30% lower than the average flux during the longer contemporaneous *BeppoSAX* observation.

Finally, combining the derived value of the ionization parameter with the luminosity of the object ( $L_{2-10} = 8.5 \times 10^{42}$  erg cm<sup>2</sup> s<sup>-1</sup>), its spectral shape ( $\Gamma \simeq 2$ ) and the inferred column density of the gas, we can write two equations linking the above, observed parameters with the density  $n_e$ , the distance  $r$  (from the nucleus) and the depth  $\Delta r$  of the gas (see Fig. 1):

$$n_e r^2 = \frac{\int_2^{10} \frac{L_\nu}{h\nu} d\nu}{4\pi c U_x} \quad n_e \Delta r = N_H \quad (6)$$

where  $r = \Delta r$  in our model (see Sect. 2). If we use the value of  $U_x$  found before to reproduce the observed lines for  $T = 10^6$  K, we get the following estimates for  $r$  and  $n_e$ :

$$n_e \simeq 2.5 \times 10^5 / f \text{ cm}^{-3}; \quad r \simeq 0.04 \cdot f \text{ pc} \quad (7)$$

These values change if we use the ionization parameters which best reproduce the observed EWs in the case of  $T = 10^5$  K and  $T = 10^7$  K (see Figs. 10 and 11), being respectively: [ $n_e \simeq 8 \times 10^5 / f \text{ cm}^{-3}$ ;  $r \simeq 0.01 \cdot f \text{ pc}$ ] and [ $n_e \simeq 8 \times 10^4 / f \text{ cm}^{-3}$ ;  $r \simeq 0.1 \cdot f \text{ pc}$ ].

This distance scale is slightly larger than that typical of the BLR (e.g. Peterson 1997). On the other hand, it is definitely smaller than the inner radius of the absorbing torus, which is of the order of parsecs (e.g. Bianchi et al. 2001). Interestingly, our estimated distance is consistent with the (poorly constrained) distance scale of warm absorbers (e.g. Otani et al. 1996; Netzer et al. 2002), but it is worth remarking that the ionization parameter required in NGC 5506 is clearly higher than that of warm absorbers.

## 5. Conclusions

We have calculated the equivalent widths of H– and He–like iron  $K\alpha$  lines from photoionized, Compton–thin matter in Seyfert galaxies, using results from MBF96 and ionization fractions estimated with CLOUDY. We have applied our calculations to NGC 5506, whose XMM–*Newton* spectrum shows a complex iron  $K\alpha$  line system, possibly composed by a neutral line and a blend of two ionized lines as those produced in our model. We found that, if this interpretation is correct, the ionized lines observed in this source can be reproduced assuming  $\log U_x \sim 0 \div 0.5$  (if  $T = 10^6$  K) and an iron overabundance of  $2 \div 3$ .

At a given gas temperature, the range of ionization parameters which produces EWs as observed in NGC 5506 is rather narrow; moreover, NGC 5506 is one of the brightest AGN in the X–ray sky. We then expect that, unless for some unknown reason the ionization parameter tends to assume values in this narrow range, in most cases these

lines will be below detectability even with XMM–*Newton* and *Chandra*, and therefore that NGC 5506 may be the exception rather than the rule. It is interesting to note that very similar iron line complexes have been observed so far by XMM–*Newton* in only two other sources, Mrk 205 (Reeves et al. 2001) and Mrk 509 (Pounds et al. 2001) where, as discussed in those papers, the origin of the ionized lines is likely to be the accretion disc.

*Acknowledgements.* We thank G. Cesare Perola for useful comments and suggestions, and the anonymous referee for his help in improving the clarity of the paper. Financial support from ASI and MIUR (under grant COFIN-00-02-36) is acknowledged.

## References

- Bianchi S., Matt G. & Iwasawa K., 2001, MNRAS, 322, 669
- Chandrasekhar S., 1960, Radiative Transfer, Dover, New York
- Ferland G., 2000, ADASS, 9, 32
- Gondoin P., Lumb D., Siddiqui H., Guainazzi M. & Schartel N., 2001, A&A, 373, 805
- Guainazzi M., Matt G., Antonelli L.A., et al., 1999, MNRAS, 310, 10
- Kaspi S., Brandt W.N., Netzer H., et al., 2001, ApJ, 554, 216
- Krolik J.H. & Kallman T.R., 1987, ApJ, 320, L5
- Lamer G., Uttley P. & McHardy I.M., 2000, MNRAS, 319, 949
- Lubinski P., & Zdziarski A.A., 2001, MNRAS, 323, L37
- Matt G., 2001, in “Issues in unification of AGNs”, eds. R. Maiolino, A. Marconi and N. Nagar, in press (astro-ph/0107584)
- Matt G., Brandt W.N. & Fabian A.C., 1996, MNRAS, 280, 823 (MBF96)
- Matt G., Guainazzi M., Perola G.C., et al., 2001, A&A, 377, L31
- Morrison R. & McCammon D., 1983, ApJ, 270, 119
- Netzer H., Chelouche D., George I.M., Turnet T.J., et al., 2002, ApJ, in press
- Otani C., Kii T., Reynolds C. S., et al., 1996, PASJ, 48, 211
- Perola G.C., et al., 2002, A&A, submitted
- Peterson B.M., 1997, Book Review: An introduction to active galactic nuclei / Cambridge U Press
- Pounds K.A., Reeves J.N., O’Brien P.T., et al., 2001, ApJ, in press (astro-ph/0112027)
- Reeves J.N., Turner M.J.L., Pounds K.A., et al. 2001, A&A, 365, L134
- Veron-Cetty M.P. & Veron P., 2001, A&A, 374, 92
- Wang T., Mihara T., Otani C., Matsuoka M. & Awaki H., 1999, ApJ, 515, 567
- Weaver K.A., 2002, in “The central kpc of starbursts and AGN: the La Palma connection”, Eds. J.H. Knapen, J.E. Beckman, I. Shlosman and T.J. Mahoney, ASP conf. series, in press (astro-ph/0108481)
- Yaqoob T., George I.M., Nandra K., et al., 2001, ApJ, 546, 759
- Yaqoob T., George I.M. & Turner T.J., 2002, In “High Energy Universe at Sharp Focus: Chandra Science”, Eds. Eric M. Schlegel and Saequ Vrtilek, in press (astro-ph/0111428)